primitive. This presents no difficulty in the non-zero-zone analysis given in Subsection 5.4.1.3 but needs consideration when two patterns are used as described in Subsection 5.4.1.2.

Unit-cell parameters may be partly or fully determined depending on the extent of knowledge of the effective camera length L and wavelength λ, and upon the type and number of patterns. The different situations are distinguished in Table 5.4.1.1 for photographic recording. Note that L is simply a magnification factor.

The accuracy of the non-zero-zone analysis described in Subsection 5.4.1.3 will depend on the influence of spiral, radial, and elliptical distortions. The camera length and wavelength need to be known to better than 1%.

For measurements made using microscope deflector systems, a knowledge of L may not be required depending on the location of the deflectors in the microscope column. Instead, the calibration factor of the deflectors, in suitable units, will replace L.

5.4.1.2. *Zero-zone analysis*

Two patterns are required that represent different sections through the reciprocal lattice. The angle of rotation p between these sections must be known, as well as the trace of the rotation axis in the plane of the pattern. Define the plane of the first pattern as the xy plane with the x axis, for convenience, coincident with the trace of the rotation axis. The coordinates x_0, y_0 of reflections in the first pattern are then measured. The coordinates x_1, y_1 of spots in the patterns rotated by p relative to the first pattern are then measured, care being taken to align the trace of the rotation axis with the x axis of the measuring equipment for each pattern. The coordinates of these reflections are then reduced to the coordinate system of the first pattern by the relations $x_0 = x_1$, $y_0 = y_1 \cos(p)$, $z_0 = y_1 \sin(p)$. The coordinates of all reflections measured are placed in a table that is scanned to extract the three shortest non-coplanar vectors. If the patterns come from dense, neighbouring zones, it is likely that these vectors define a primitive cell.

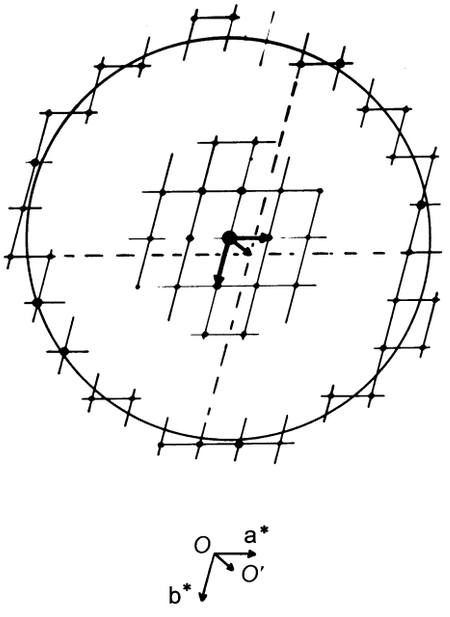

Fig. 5.4.1.2. A diffraction pattern with the crystal oriented at a zone axis. The lower diagram shows the zero-zone vectors $\mathbf{a}^*$ and $\mathbf{b}^*$, and OO', the projection on the xy plane of $\mathbf{c}^*$.

5.4.1.3. *Non-zero-zone analysis*

One pattern with well defined Laue zones taken at an arbitrary zone allows the recovery of a third vector not in the plane of the pattern. First find the components for the two shortest zero-zone vectors $\mathbf{a}^*$ and $\mathbf{b}^*$ (see Fig. 5.4.1.2). For the third vector, measure the x and y coordinates of a non-zero-zone vector. These are then transformed to components in the coordinate system defined by the two shortest vectors of the zero zone. Then the fractional part of each transformed component is taken. If the vector comes from a Laue zone of order n, these fractional parts must be divided by n. A transformation back to Cartesian coordinates gives the x and y components of the third vector $\mathbf{c}^*$, point O' in Fig. 5.4.1.2. In practice, it is best to measure a set of vectors at roughly equal angles around the zone so that an average can be taken to improve accuracy.

For certain space groups and special orientations, it is possible for half of the zero-zone reflections to be absent. If sufficient non-zero-zone vectors have been measured, two different vectors OO' should be found. New axes $(\mathbf{a}^* + \mathbf{b}^*)/2$ and $(\mathbf{a}^* - \mathbf{b}^*)/2$ must then be chosen and the x and y coordinates of $\mathbf{c}^*$ recalculated.

The z component of $\mathbf{c}^*$ is obtained (Fig. 5.4.1.1) from

$$c_z^* = L[1 - 1/(1 + r^2/L^2)^{1/2}]/n,$$

where r is the radius of the Laue circle of order n.

We now have the orientation matrix $\boldsymbol{UB}$ as

$$\boldsymbol{UB} = \begin{pmatrix} a_x^* & b_x^* & c_x^* \\ a_y^* & b_y^* & c_y^* \\ 0 & 0 & c_z^* \end{pmatrix},$$

and the measurement of the pattern is complete.

After transformation of the axes defined by $\boldsymbol{UB}$ to the Bravais axes, the inverse of the resulting $\boldsymbol{UB}_{\text{Bravais}}$ will index the pattern using

$$\begin{pmatrix} h \\ k \\ l \end{pmatrix} = \boldsymbol{UB}_{\text{Bravais}}^{-1} \begin{pmatrix} x \\ y \\ z \end{pmatrix}.$$

5.4.2. Kikuchi and HOLZ techniques (By A. Olsen)

Lattice-parameter determination based on selected-area electron-diffraction patterns requires accurate calibration of the camera constant K. This constant depends on the electron wavelength λ and the camera length L and is given by $K = \lambda L$. Because the camera constant cannot be determined with sufficient accuracy in a transmission electron microscope, a number of methods for determination of lattice parameters (or electron wavelength)

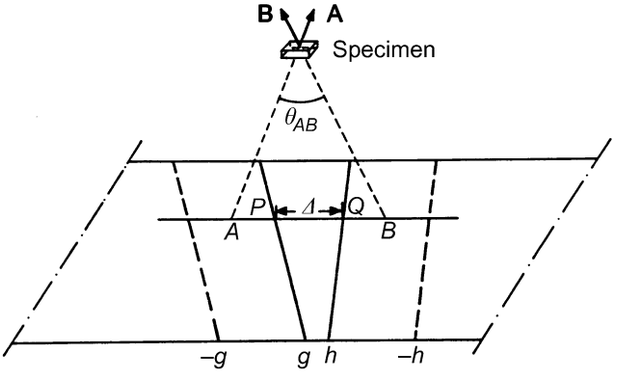

Fig. 5.4.2.1. Schematic diagram showing the geometry of a Kikuchi pattern.

have been developed based on Kikuchi or HOLZ (high-order Laue zone) lines (Uyeda, Nonoyama & Kogiso, 1965; Høier, 1969; Olsen, 1976*a*; Jones, Rackham & Steeds, 1977). In these methods, the lattice parameters can be determined, provided the electron wavelength is known (or *vice versa*) without knowing the value of K.

In the method of Uyeda *et al*. (1965), the electron wavelength can be determined from a single Kikuchi pattern provided that the lattice parameters of the crystal are known. Fig. 5.4.2.1 illustrates the geometry involved in the method. **A** and **B** are two zone axes of the specimen. The pairs of Kikuchi lines g, $-g$ and h, $-h$ belong to the zones **A** and **B**, respectively. The points P and Q are the intersections of the Kikuchi lines g and h with the line AB.

As a first approximation, the wavelength of the electrons is given by

$$\lambda = \theta_{AB}/[(1/2d_P) + (1/2d_Q) + (\Delta/D)(1/d)], \qquad (5.4.2.1)$$

where D is the measured distance between the two Kikuchi lines in either of the pairs and d is the corresponding interplanar spacing. θ_{AB} is the angle between the zone axes **A** and **B**. When the Kikuchi pattern is indexed, θ_{AB} and d can be calculated from the known lattice parameters of the specimen. d_P and d_Q are effective interplanar spacings and are given by

$$\begin{aligned} d_P &= d_g \sin\varphi_g, \\ d_Q &= d_h \sin\varphi_h; \end{aligned} \qquad (5.4.2.2)$$

d_g and d_h are the interplanar spacings corresponding to g and h, respectively. The angle φ_g (or φ_h) is the angle between the lattice plane g (or h) and the plane defined by **A** and **B**. These angles are given by

$$\begin{aligned} \sin\varphi_g &= \mathbf{g} \times (\mathbf{A} \times \mathbf{B})/(|\mathbf{g}| \cdot |\mathbf{A} \times \mathbf{B}|), \\ \sin\varphi_h &= \mathbf{h} \times (\mathbf{A} \times \mathbf{B})/(|\mathbf{g}| \cdot |\mathbf{A} \times \mathbf{B}|). \end{aligned} \qquad (5.4.2.3)$$

The values of d_P and d_Q to be used in (5.4.2.1) can be calculated from (5.4.2.2) and (5.4.2.3).

If Δ and D are measured on the photographic plate or a print of any magnification, the electron wavelength can be calculated by using (5.4.2.1). Only the ratio (Δ/D) is required for the determination of λ. The distance AB is not required. The points A and B are used only to fix the points P and Q. A and B do not need to fall inside the photographic plate when a Kikuchi pattern is symmetrical across the line AB, because in such cases P and Q can be determined from intersections of Kikuchi lines that are symmetrical with each other. The expression for λ in (5.4.2.1) is only a first approximation. More accurate expressions can be found in the paper by Uyeda *et al*. (1965).

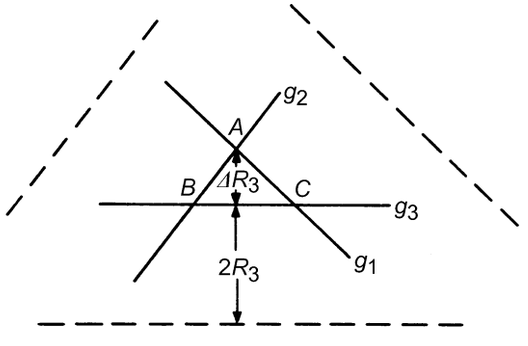

Fig. 5.4.2.2. Schematic diagram of three Kikuchi lines that nearly intersect at the same point.

A simpler and more accurate method has been developed by Høier (1969). He showed that in the cubic case it is possible to determine the ratio between the lattice parameter a and the electron wavelength λ with a relative accuracy of 0.1%. Only two quantities have to be measured on the photographic plate or a print at any magnification: the height of a triangle formed by three Kikuchi lines and one separation between a defect–excess line pair (Fig. 5.4.2.2). If three indexed Kikuchi lines g_i intersect at the same point on a photographic plate, the following equations can be derived from Bragg's law:

$$2\mathbf{g}_i\mathbf{K}_i = -|\mathbf{g}_i|^2, \quad i = 1, 2, 3. \qquad (5.4.2.4)$$

In addition, the length of **K** is equal to the electron wavelength

$$|\mathbf{K}_i| = 1/\lambda_i, \qquad (5.4.2.5)$$

where the wavelength is written λ_i for generality (for electrons, $\lambda_i = \lambda$). If the Kikuchi lines g_i do not belong to the same zone, (5.4.2.4) and (5.4.2.5) can be solved and a/λ determined.

Exact triple intersections are rare. A practical method as proposed by Høier (1969) is therefore based on three lines that nearly intersect at the same point (Fig. 5.4.2.2). The dimensions of the triangle ABC in Fig. 5.4.2.2 change with λ. Let us assume that only the wavelength in the beam giving the g_3 reflection varies. The increment $\Delta\lambda_3$ necessary to shift the line g_3 to A is then determined by

$$\lambda_3 = \lambda + \Delta\lambda_3 \sim \lambda(1 + \Delta R_3/R_3). \qquad (5.4.2.6)$$

By measuring the height in the triangle ABC and the line separation $2R_3$, the wavelength to be used in (5.4.2.5) can be calculated and the ratio a/λ determined. Care must be taken to avoid areas where the lines are displaced from kinematical positions owing to dynamical interactions.

The method of Høier (1969) for cubic crystals was later extended to lower-symmetry cases (triclinic) by Olsen (1976*a*), who also developed computer programs for least-squares refinement of the lattice parameters. The derivation of the equations for the procedure is carried out in the following in a way slightly different from that described by Olsen (1976*a*).

If three Kikuchi lines $\mathbf{g}_i(h_i, k_i, l_i)$ not belonging to the same zone intersect at the same point on the photographic plate, the direction **K** from the origin of the Ewald sphere to the intersection point of the Kikuchi lines is given by Bragg's law:

$$2\mathbf{g}_i\mathbf{K} = -|\mathbf{g}_i|^2, \quad i = 1, 2, 3. \qquad (5.4.2.7)$$

The length of the vector **K** is given by

$$|\mathbf{K}| = 1/\lambda, \qquad (5.4.2.8)$$

where λ is the electron wavelength.

Because triple intersections are rare, a practical method is therefore based on three lines that nearly intersect at the same point, as proposed by Høier (1969). In order to obtain an exact intersection, one of the lines can be changed from $\mathbf{g}_i$ to $\mathbf{g}_i + \Delta\mathbf{g}_i$, where $\Delta\mathbf{g}_i$ is a vector approximately parallel to $\mathbf{g}_i$. For this Kikuchi line (in the following assumed to be line no. 3), the Bragg condition (5.4.2.7) gives

$$2(\mathbf{g}_3 + \Delta\mathbf{g}_3)\mathbf{K} = -(\mathbf{g}_3 + \Delta\mathbf{g}_3)^2. \qquad (5.4.2.9)$$

For a pair of Kikuchi lines, the simple relation

$$2\Delta\mathbf{g}_3 = (\Delta R_3/R_3)\mathbf{g}_3 \qquad (5.4.2.10)$$

holds, where $2R_3$ is the line separation measured on the photographic plate of the centres of the two Kikuchi lines. ΔR_3 is the shift (measured on the plate) in the position of one of the lines in order to obtain an exact triple intersection.

Substitution of (5.4.2.10) into (5.4.2.9) gives

$$2\mathbf{g}_3\mathbf{K} = -|\mathbf{g}_3|^2(1 + \Delta R_3/R_3). \qquad (5.4.2.11)$$

From n measurements of intersections, the following equations are obtained:

$$h_{ji}u_j + k_{ji}v_j + l_{ji}w_j = -(1/2)(1/d_{ji})^2(1 + \delta_{i3}\Delta R_{j3}/R_{j3}), \quad i = 1, 2, 3, \quad j = 1, 2, \ldots, n, \qquad (5.4.2.12)$$

where h_{ji}, k_{ji}, l_{ji} are the indices (given in reciprocal space) of the Kikuchi lines, δ_{i3} is the Kronecker delta, u_j, v_j, w_j are the indices (given in real space) of the direction $\mathbf{K}_j$ to the intersection number $\mathbf{j}$, and d_{ji} is the interplanar spacing corresponding to the reflection h_{ji}, k_{ji}, l_{ji} and can be expressed in terms of the cell dimensions in real space. The length of the $\mathbf{K}_j$ vectors can also be expressed in terms of the lattice parameters in real space a, b, c, α, β, and γ as

$$|\mathbf{K}_j| = (u_j^2a^2 + v_j^2b^2 + w_j^2c^2 + 2u_jv_j\,ab\cos\alpha + 2u_jw_j\,ac\cos\beta + 2v_jw_j\,bc\cos\gamma)^{1/2}. \qquad (5.4.2.13)$$

Equations (5.4.2.12) can be solved with respect to u_j, v_j, w_j, and $\mathbf{K}_j$ can then be expressed in terms of the lattice parameters by substituting the expressions for u_j, v_j, w_j from (5.4.2.12) into (5.4.2.13).

If the number of intersections is greater than the number of unknown lattice parameters, a least-squares-refinement procedure can be used. This involves minimizing the function

$$Q = \sum_j (|\mathbf{K}_j| - 1/\lambda)^2. \qquad (5.4.2.14)$$

Because the expression for Q is non-linear in the lattice parameters, a refinement procedure can be used to solve the equations derived from (5.4.2.14) using the least-squares procedure. The accuracy in the lattice parameters or wavelength can be found by statistical methods. A computer program for refinement of the lattice parameters (or electron wavelength) is available (Olsen, 1976*b*). In this program, some of the lattice parameters can be held constant or kept equal during the refinement.

Methods based on measurements of distances between zone axes (poles) in the Kikuchi patterns (Thomas, 1970) are not very accurate because optical distortions make long-distance measurements inaccurate on the photographic plate or a magnified print.

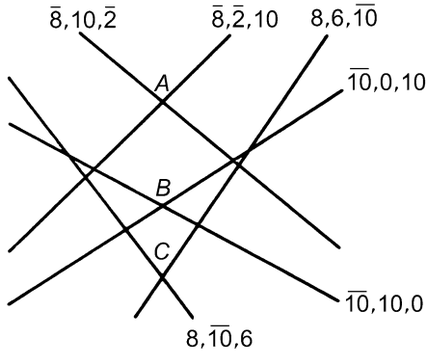

Fig. 5.4.2.3. Schematic diagram showing the indexing of the most prominent lines in the selected-area channelling pattern near the [111] zone of Si. Accelerating voltage: 25 kV.

The methods by Høier (1969) and Olsen (1976*a*) are based on 'near intersections'. Better accuracy may be obtained if the high voltage can be varied in order to obtain exact intersections. A simple method for determination of lattice parameters can be applied for crystals with symmetry as low as orthorhombic (Gjønnes & Olsen, 1984). The method is a simplified version of the Uyeda *et al.* (1965) method. If two parallel Kikuchi lines belonging to different zones overlap, then:

$$2\mathbf{g}_i\mathbf{K} = -|\mathbf{g}_i|^2, \quad i = 1, 2; \qquad (\mathbf{g}_1 \times \mathbf{g}_2)\mathbf{K} = 0, \quad |\mathbf{K}| = 1/\lambda. \qquad (5.4.2.15)$$

These equations can be solved to give the ratio between lattice parameter and electron wavelength.

A simple, rapid procedure for accelerating-voltage (or electron-wavelength) determination of a transmission electron microscope has been described by FitzGerald & Johnson (1984). In their method, it is necessary to measure the ratio of two easily found distances between points defined by the intersections of Kikuchi lines near the ⟨111⟩ zone of a silicon crystal. It is not necessary to index the Kikuchi lines, because the method is based on (*a*) a particular crystal and (*b*) an easily recognizable crystal orientation, and because the points between which distances need to be measured are specified in their paper and can be easily found. Polynominals for converting the distance measurements both to electron wavelength and to accelerating voltage are given for the range from 100 to 200 kV. A 300 K temperature change must occur (temperature coefficient of 3×10^{-6} K) before the error in the lattice parameter of silicon due to thermal expansion becomes significant.

A method for measuring small local changes in the lattice parameter of bulk specimens based on selected-area channelling patterns has been described by Walker & Booker (1982). The method utilizes the small changes in the position of high-index channelling lines due to small changes in the lattice parameters, and is based on scanning electron microscopy (SEM). The method is rapid and convenient, is suitable for bulk specimens, and can be applied to areas only a few micrometres across. The method has been used for Si and GaP and is in this case based on the intersection of pairs of $\bar{8}$,10,$\bar{2}$, $\bar{1}0$,10,0, 8,$\bar{1}0$,6 type lines (the points *A*, *B*, and *C* in Fig. 5.4.2.3). Selected-area channelling patterns from Si and GaP obtained under precisely the same conditions have the same characteristic array of lines, but with slightly different distances *AB* and *BC*. The detection limit of this method is at present 3 parts in 10^4.

When a small electron probe is used to illuminate a crystal, as in convergent-beam electron diffraction (CBED), very fine lines are often found in the diffraction discs (Steeds, 1979). These lines are called HOLZ lines. They are due to upper-layer diffraction effects and can be used in lattice-parameter determination (Rackham, Jones & Steeds, 1974; Jones, Rackham & Steeds, 1977). For highest accuracy, relatively thick crystals are required. The limitation to the accuracy is set either by the weakness of the lines or by energy losses in the specimen. Relative changes in the lattice parameters can be measured to an accuracy of 1 part in 10^4, whereas the accuracy in the absolute determination of lattice parameters is typically of an order of magnitude worse. The lattice parameters can be measured from crystal regions as small as 20 nm in diameter with an accuracy better than 1 part in 10^3. If more accurate results are desired, it is necessary to make measurements on lines that are not affected by interactions between HOLZ reflections.

references